Hindawi
Journal of Chemistry
Volume 2023, Article ID 7465722, 19 pages
https://doi.org/10.1155/2023/7465722

Research Article

Fast and Selective Adsorption of Au (III) from the Waste Printed Circuit Boards Using a Low-Cost Adsorbent: Optimization by Central Composite Design Based on Response Surface Methodology

Farideh Zandi-Darehgharibi,[1] **Hedayat Haddadi**,[1] **and Arash Asfaram**[2]

[1]*Department of Chemistry, Faculty of Basic Sciences, Shahrekord University, Shahrekord, Iran*
[2]*Medicinal Plants Research Center, Yasuj University of Medical Sciences, Yasuj, Iran*

Correspondence should be addressed to Hedayat Haddadi; hedayathaddadi@yahoo.com

Received 18 May 2023; Revised 3 August 2023; Accepted 22 August 2023; Published 4 September 2023

Academic Editor: Doina Humelnicu

A low-cost new green adsorbent (GA) was synthesized by tannin-rich pomegranate peel powder and formaldehyde for the fast and selective recovery of Au (III). It was characterized by Fourier transform infrared spectroscopy (FT-IR), Brunauer–Emmett–Teller (BET), elemental analysis (CHN), field emission scanning electron microscopy (FE-SEM), and energy-dispersive X-ray spectroscopy (EDS) (FE-SEM-EDS-mapping). The optimal values of influential factors were defined using a central composite design based on the response surface methodology (CCD-RSM). Adsorption properties were investigated by the kinetic, isotherm, thermodynamic, and interference of coexisting metal ions at optimum conditions. The experimental adsorption percentage with three repetitions under the optimized conditions such as pH = 2, adsorbent mass = 23 mg, Au (III) concentration = 32 mg L^{-1}, and contact time = 30 min was 97% and the highest adsorption capacity of the GA was 315.450 mg g^{-1}. The adsorption isotherm and kinetic were clarified by the Freundlich ($R^2 = 0.952$) and pseudo-second-order ($R^2 = 0.998$) models. The thermodynamic study ($\Delta S^\circ > 0$, $\Delta H^\circ > 0$, and $\Delta G^\circ < 0$) revealed that Au (III) adsorption via GA was a facile, endothermic, and spontaneous process. The adsorption mechanism could be an electrostatic interaction and reductive adsorption. A small amount of GA (23 mg) adsorbed gold selectively and rapidly (30 min) from coexisting metals present in the waste printed circuit board (PCB) such as Ag, Al, Si, Zn, Pb, Ba, Ni, Ca, Mo, Co, Cr, Mn, Cu, Mg, Fe, and W. These results confirm the use of low-cost and high-efficiency GA to fast and selectively recover gold from waste PCBs.

1. Introduction

Gold is used in the manufacture of various electronic devices such as cell phones, televisions, and computers due to its physical, chemical, and conductive properties. With the advancement of technology, new electronic devices are replacing older ones every day, thus producing electronic waste (e-waste). Printed circuit boards (PCBs) as one of the electronic waste contain 350 grams of gold per ton, while the gold ore contains 5 to 30 grams of this precious metal per ton. As this e-waste contains much larger amounts of gold than the gold ore, it may be considered a secondary source of gold [1–7]. Due to the limited natural resources of gold, it is of paramount importance to recover this precious metal from e-waste. Economically, the recovery process should be as follows: gold is isolated very selectively from the base metals such as iron, copper, and zinc that are often present in disproportionate amounts with this precious metal [8]. Therefore, there is a need to develop efficient technologies for the recovery of gold from a wide range of secondary sources.

At present, there are various processes such as the use of metal-organic frameworks, ion exchange resins, solvent extraction, and adsorption with biosorbents to recover gold.

Among these processes, the adsorption process with natural adsorbents is simpler and more effective. There are many reports on the use of natural wastes such as persimmon peel, orange waste, banana peel, and lemon peel due to their phenolic compounds and tannins content to recover gold. In other words, phenolic compounds and tannins have a high affinity for gold due to their hydroxyl groups. One of the most important advantages of using biological waste for gold recovery is that they are easily available in large quantities at low cost. Environmental compatibility, degradability, and renewability are other advantages of them [8–18].

Factors such as solution pH, contact time, initial concentration, and adsorbent dose have been found to affect adsorbent performance. The correct understanding of the interaction of these factors is thus necessary to optimize the adsorption condition. Experimental design is a useful technique to optimize effective parameters. To investigate independent parameters and their interactions that are effective in the adsorption process, central composite design-response surface methodology (CCD-RSM) is used. CCD is a useful statistical technique with a small number of tests [19–28].

Considering that the process of recovering precious metals should be simple and cost-effective from the economic point of view, a low-cost and readily accessible natural adsorbent was synthesized from pomegranate peel tannins with a simple and facile process as an adsorbent for fast and selective recovery of gold. CCD-RSM was used to determine the optimal values of the parameters affecting the gold adsorption process to reach the maximum amount of adsorption. The synthesis of this adsorbent and its combination with the experimental design technique to optimize the effective parameters in gold recovery have been performed for the first time in this study. Moreover, the isotherm, kinetic, thermodynamic, and interference of coexisting metal ions were investigated under optimum conditions.

2. Methodology and Analysis

2.1. Materials and Chemicals. Tannin-rich pomegranate peel was obtained from the Sheyvand village of Izeh City, Iran. NaOH, HNO_3, HCl, HAuCl4·xH2O, Folin–Ciocalteu's phenol reagent, formaldehyde, solvents, and other chemicals were purchased from Merck. Waste PCB was obtained from Shahrekord University.

2.2. Quantifying Total Phenolic Content (TPC) of Pomegranate Peel. The Folin–Ciocalteu methodology was employed to define the total phenol content of tannin-rich pomegranate peel [29]. Tannin-rich pomegranate peel(0.01 g) was dissolved in 60% methanol (10 mL). In the next step, 10% Folin–Ciocalteu reagent (0.5 mL) was added to a portion (2 mL) of the previous solution (10 mg/mL). The mixture was placed for 5 min at an ambient temperature and then mixed with the Na_2CO_3 solution (7.5% w/v) (0.4 mL). The sample was kept in the darkness for 30 min, and the UV-Vis Spectrophotometer defined the absorbance at 765 nm. Gallic acid was used as the standard, and the data were computed as milligrams of gallic acid equivalent per gram dry weight (mg GAE/g DW).

2.3. Preparation and Characterization of the Adsorbent. Tannin-rich pomegranate peel powder (30 g) was dissolved in 65 mL of NaOH fresh solution (0.25 M) at room temperature and 6 mL of 37% formaldehyde solution was then added to it. Then, the mixture was heated at 353 K. After 12 hours, the product was filtered and crushed and then rinsed several times with deionized water. The HNO_3 solution (0.05 M) was used to remove the unreacted materials. After that, the product was rinsed with distilled water. Finally, it was dried at 338 K for 24 hours [4]. This product was green adsorbent (GA) and used for adsorption tests. To characterize the product obtained before and after adsorption, FTIR, BET, CHN, and FE-SEM-EDS-mapping were performed.

2.4. Experimental Design. Design Expert software version 13 was used to optimize the factors. The optimal values of factors were determined using the CCD-RSM. CCD was run for each factor at five levels ($-\alpha$, low (−1), center (0), high (+1), and $+\alpha$) and 21 experiments were performed in the small mode. Ranges of factors, including solution pH (1–5), adsorbent mass (7–35 mg), Au (III) concentration (20–100 mg L^{-1}), and contact time (10–50 min) are shown in Table S1. Using the optimal values determined by the CCD, kinetic, thermodynamic, adsorption isotherm, and interference of coexisting metal ions were investigated.

2.5. Adsorption Experiments. To investigate factors affecting Au (III) adsorption by GA, 21 experiments designed by CCD were conducted in aqueous solutions with different pH values, adsorbent doses, contact times, and Au (III) concentrations using a thermostatic shaker at 200 rpm. The solution obtained by filtering the heterogeneous mixture was collected for inductively coupled plasma optical emission spectroscopy (ICP-OES) analysis. The percentage of Au (III) adsorption by GA was calculated using the initial and equilibrium concentrations through the following equation:

$$\%\, A = \frac{C_i - C_t}{C_i} \times 100, \tag{1}$$

where C_i and C_t are Au (III) initial and equilibrium concentrations in mg L^{-1}.

In addition, the experiments of kinetic, thermodynamic, isotherm, and coexisting metal ions were performed using the optimal values obtained from CCD for effective factors.

2.6. Aqua Regia Digestion of Real Sample (Waste PCB). First, the waste PCB was placed in the furnace with a high temperature of 1023 K to burn plastic, etc., for 4 hours. The melted metals were then turned into uniform fine particles by the planetary mill. Five grams of powdered metals were

digested by 56 mL of aqua regia reverse (14 mL of 37% w HCl with 42 mL of 69% w HNO_3). The mixture was heated to 473 K for 2 hours. After cooling, the mixture was filtered [30]. The concentration of metals in the solution at pH = 2 (Au = 30.12, Ag = 6, Al = 8423, Ba = 133, Ca = 1160, Co = 2, Cr = 59, Cu = 8196, Fe = 744, Mg = 71, Mn = 13.6, Mo = 1, Ni = 176, Pb = 16.3, Si = 7, W = 0.3, and Zn = 40 mg L^{-1}) was measured using ICP-OES.

3. Results and Discussion

3.1. Adsorbent Characterization

3.1.1. TPC in Pomegranate Peel. The TPC of pomegranate peel was 168.00 ± 5.75 mg GAE/g DW. This measurement provides evidence on considerable quantities of phenolic compounds in the pomegranate peel that have two major components, carbon and oxygen, in their structure. The TPC of the two types of pomegranate peel was reported to be 102.9 ± 0.9 and 85.9 ± 1.3 mg GAE/g DW [31]. Several studies have found pomegranate peel to be rich in phenolic compounds [32–37].

3.1.2. FTIR Analysis. Figure 1 shows the FTIR spectra of tannin-rich pomegranate peel powder and GA. The broad peaks at 3600–3100 cm^{-1} exhibit the stretching vibration of the O-H group of phenol [38]. The peaks at 1450 and 1446 cm^{-1} correspond to the C-C of the ring [5, 39, 40]. The peaks in the narrow area of 1390–1310 cm^{-1} are associated with O-H phenolic bending. The peaks at 1232 and 1033 cm^{-1} display the stretching vibrations of the carbonyl group (C-O) [3, 4, 31]. These data confirm that the pomegranate peel is rich in phenolic compounds which have carbon and oxygen as their two main elements. The reaction between formaldehyde and pomegranate peel tannin leads to methylene bridges. The slight peaks at 2937 and 2931 cm^{-1} are associated with the C-H stretching of phenolic rings of pomegranate peel tannin and methylene bridges [4, 41, 42]. The peaks at 910–740 cm^{-1} display deformation vibrations of the C-H bond in phenolic rings and the intensity of this area has dwindled due to the cross-links between pomegranate peel tannin and formaldehyde (Figure 1(b)) [4].

3.1.3. FE-SEM, BET, CHN, and EDS-Mapping Analysis. FE-SEM examination was performed to investigate the morphology of the surface (Figure 2). The images of FE-SEM at diverse magnifications showed that GA has a rough, nonuniform, and porous surface. Moreover, the GA surface area was computed by BET and the outcomes displayed a surface area of 2.115 m^2g^{-1}. In addition, the pore volume and the mean pore diameter of the GA were 0.0063 cm^3g^{-1} and 11.964 nm, respectively (Table 1). BET results implied that the GA can be mesoporous and this is in agreement with the reports [43, 44]. This mesoporous and free form may lead to the adsorption of Au (III) ions (Figures 2(a)–2(c)). After adsorption, diverse outcomes emerged from the GA composite, indicating that Au (III) ions are hooked onto the rough and porous surface of the GA to cover its surface (Figures 2(d)–2(f)). Furthermore, the agglomeration of Au onto the GA surface is also proved with EDS-mapping (Figures 3(c) and 3(d)).

CHN elemental analysis of GA indicates that carbon (47.49%), hydrogen (4.91%), and nitrogen (1.17%) are its composition (Table 2). Figure 3 shows the results of EDS-mapping of the GA before and after loading Au (III) on it. EDS-mapping elemental analysis showed the existence and percentage of the weight of C (67.0%) and O (33.0%) in the GA before adsorption (Figures 3(a) and 3(b)). Moreover, carbon (30.6%–51.40%) and oxygen (46.21%–61.7%) as the two main components of pomegranate peel were reported by researchers [43–48]. The existence and percentage of the weight of C (69.9%), O (29.7%), and Au (0.4%) after adsorption are shown in Figures 3(c) and 3(d). The EDS-mapping elemental analysis confirmed the adsorption of Au (III) ions via the GA surface.

3.2. Factors Optimization to Reach the Maximum Au (III) Adsorption. Optimization is obtaining the maximum effect of several independent variables and their simultaneous interactions on a process [21]. Therefore, to achieve maximum Au (III) adsorption on the GA, optimization was accomplished by CCD-RSM, and the optimal amount of factors was determined. The results of CCD are shown in Table S2. Under the conditions of pH = 2, adsorbent mass = 23 mg, Au (III) concentration = 32 mg L^{-1}, and contact time = 30 min, the adsorption percentage was predicted to be greater than 98% with the desirability of 1.0. The desirability is evaluated in a range of 0 to 1, with 0 indicating undesirable conditions, and 1 showing optimal desirable conditions. Three repetitions were conducted with the acquired optimal values by CCD, to confirm the adsorption percentage predicted by it. The experimental adsorption percentage was 97%, which was in good compromise with the anticipated amount.

3.3. Statistical Analysis. Table S3 shows the analysis of variance (ANOVA) results and model summary statistics. As shown in Table S3, the significance of the model is given by the F-value of 221.42. Due to the p value of the model being less than 0.0500, the A, B, C, D, AC, AD, BD, C^2, and D^2 terms of the model are significant. The F-value of 1.81 reveals that the lack of fit is not significant relative to the pure error, and the nonsignificant lack of fit is good. The anticipated R^2 of 0.8926 is in good accord with the adjusted R^2 of 0.9936; i.e., the difference is less than 0.2. Adequate precision calculates the signal-to-noise proportion and a ratio of more than 4 is acceptable. The proportion of 52.347 shows an adequate signal.

3.4. Influence of Interaction of Variables on Au (III) Adsorption. The simultaneous effect of the influential variables including pH, adsorbent mass, Au (III) concentration, and contact time on Au (III) adsorption by GA was evaluated. Contour plots and three-dimensional response surfaces of Au (III) adsorption via GA are shown in Figure 4.

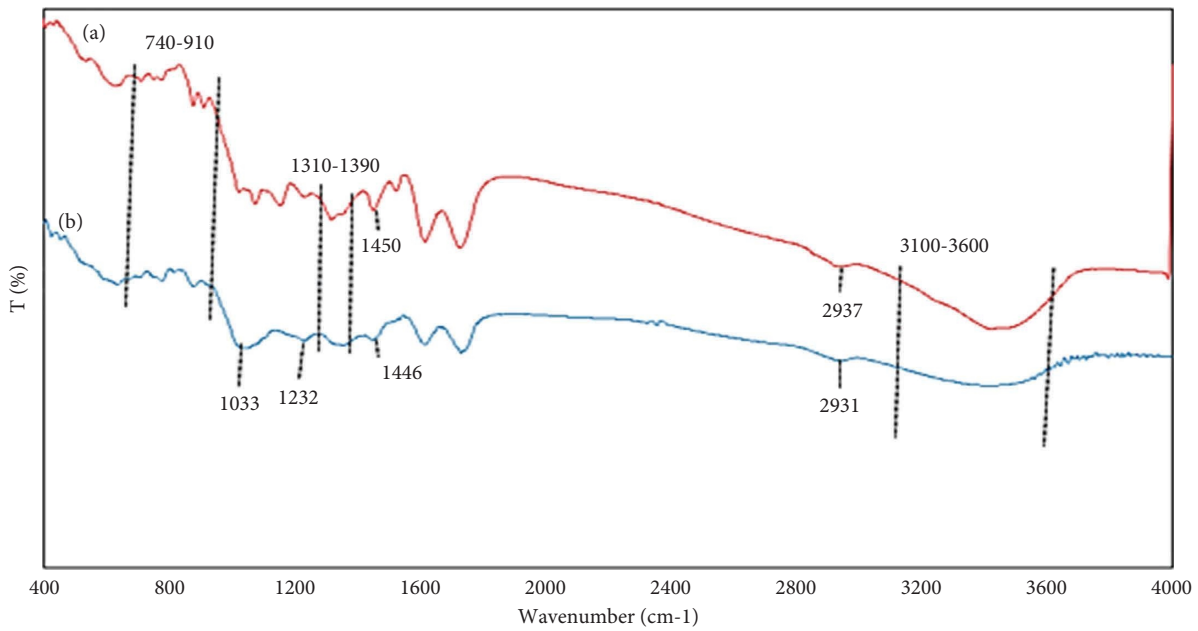

Figure 1: FTIR spectra of tannin-rich pomegranate peel powder (a) and GA (b).

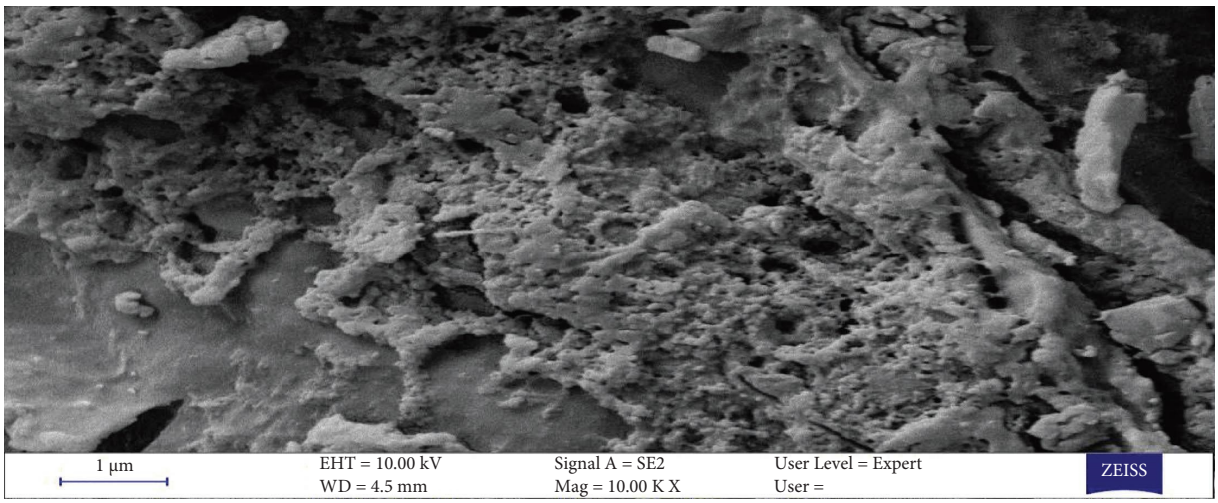

(a)

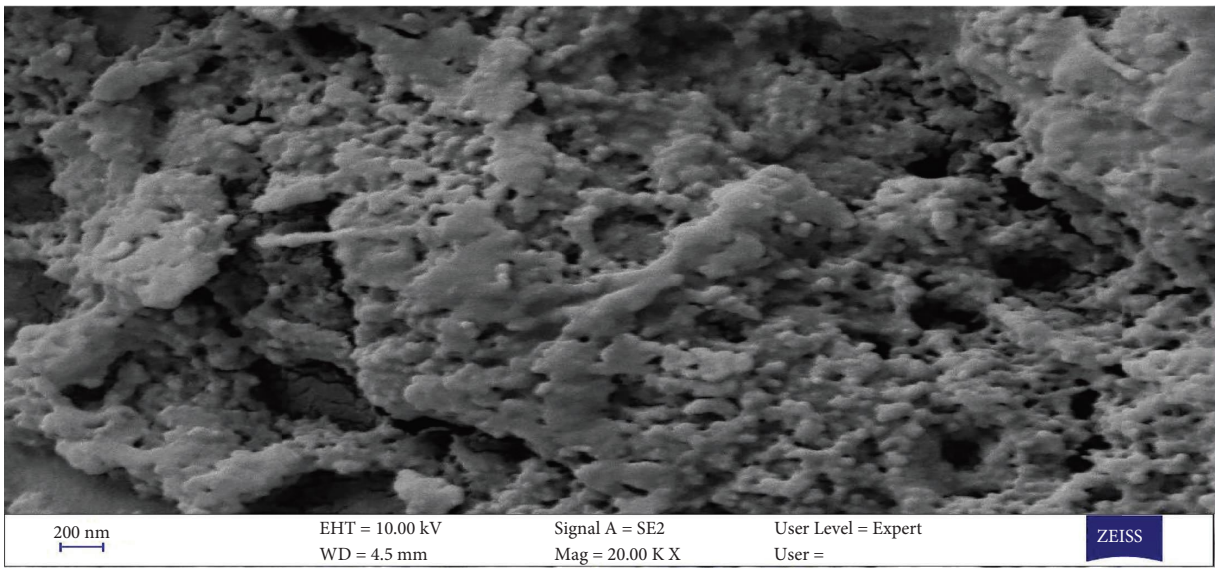

(b)

Figure 2: Continued.

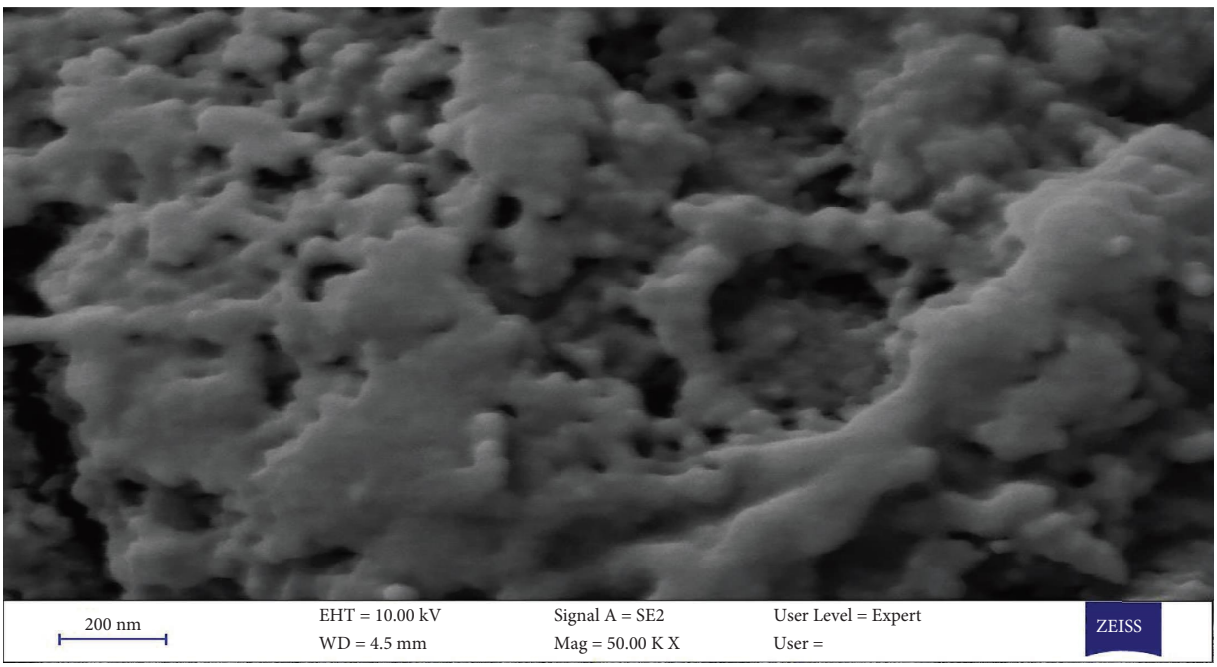

(c)

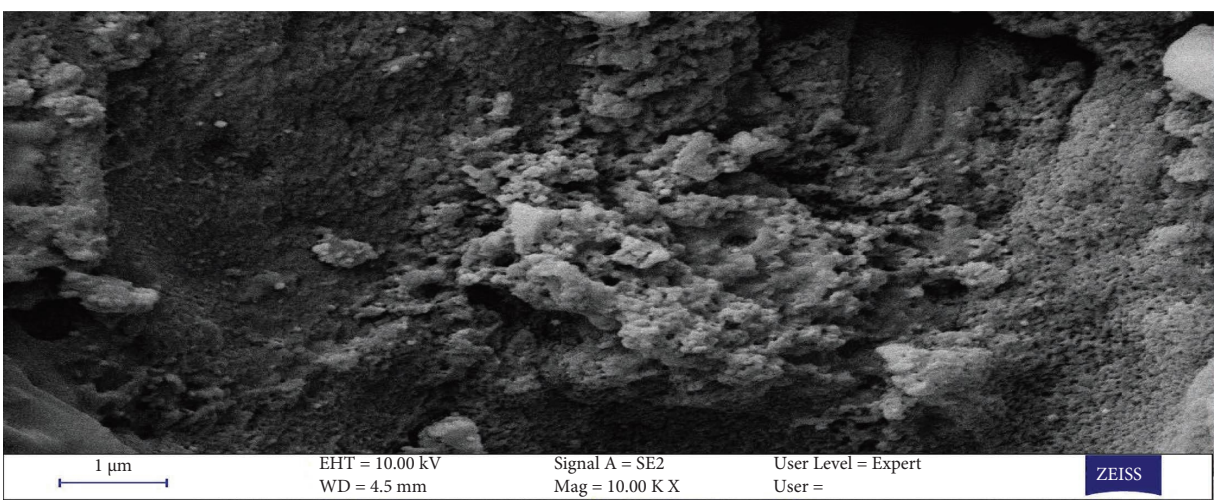

(d)

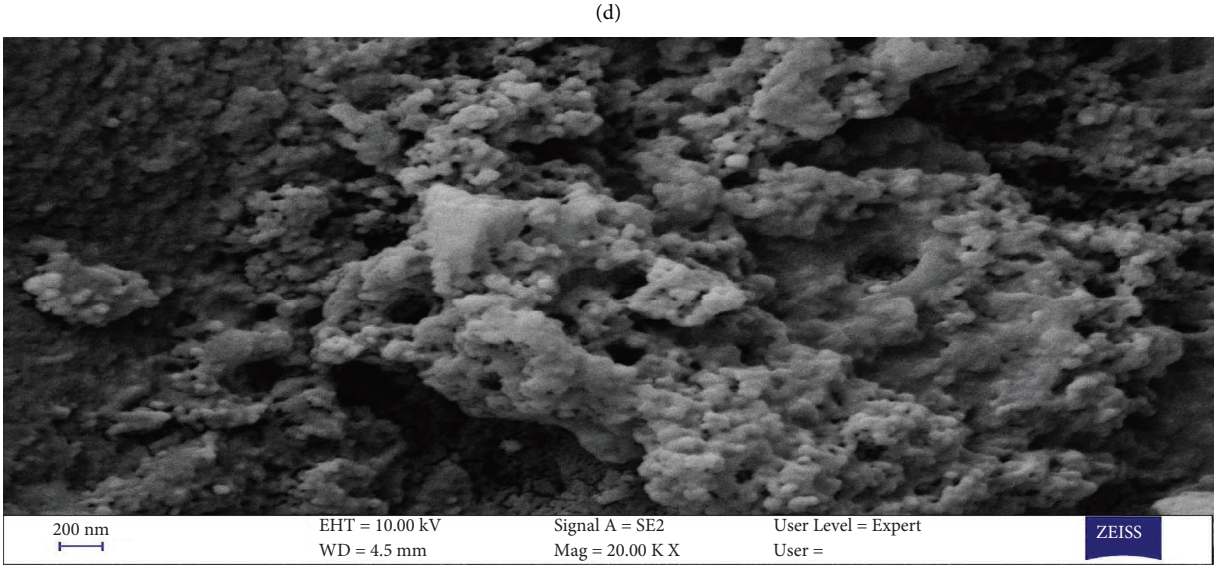

(e)

Figure 2: Continued.

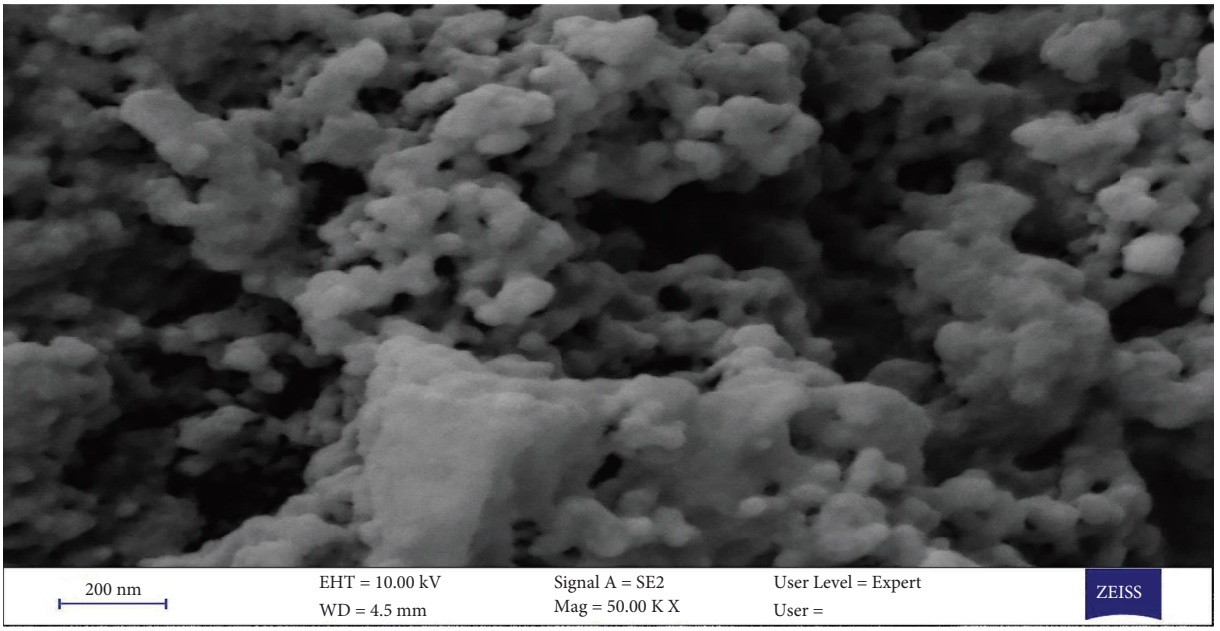

(f)

Figure 2: FE-SEM of the GA before loading Au (III) (a–c) and after loading Au (III) (d–f) on it.

Table 1: BET characteristics of the GA.

Adsorbent	BET surface area (m^2g^{-1})	Total pore volume (cm^3g^{-1})	Mean pore diameter (nm)
GA	2.115	0.0063	11.964

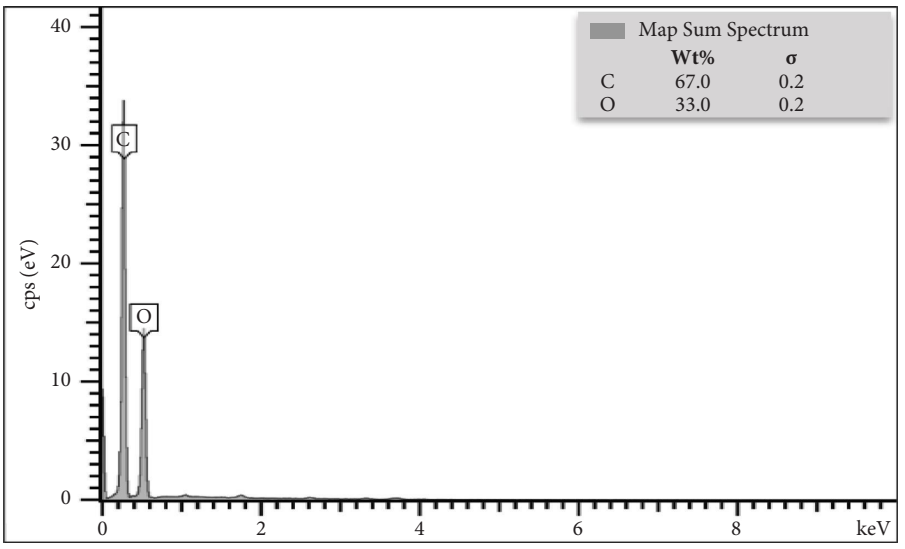

(a)

Figure 3: Continued.

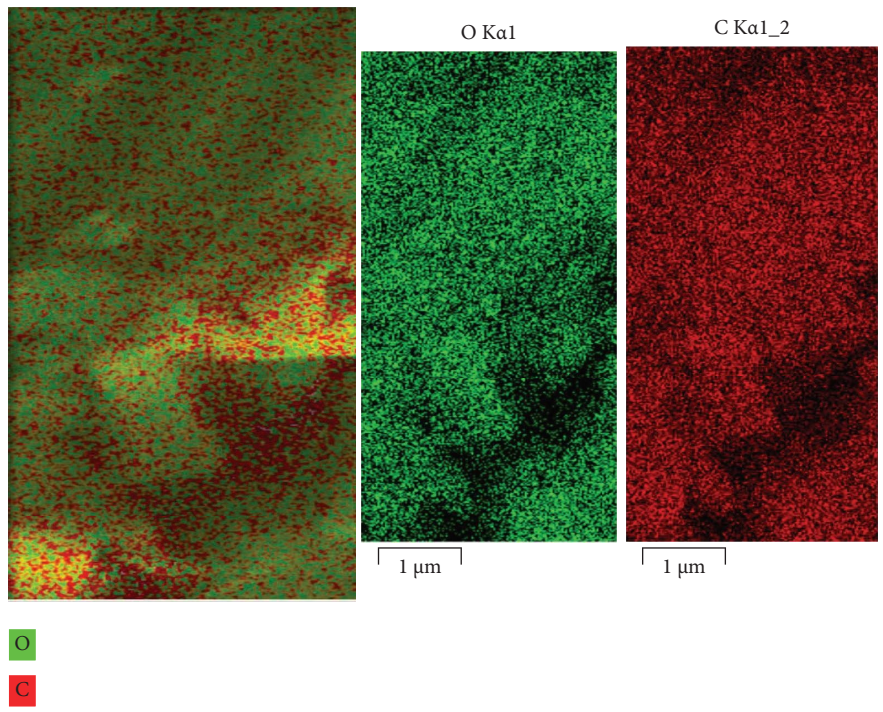

(b)

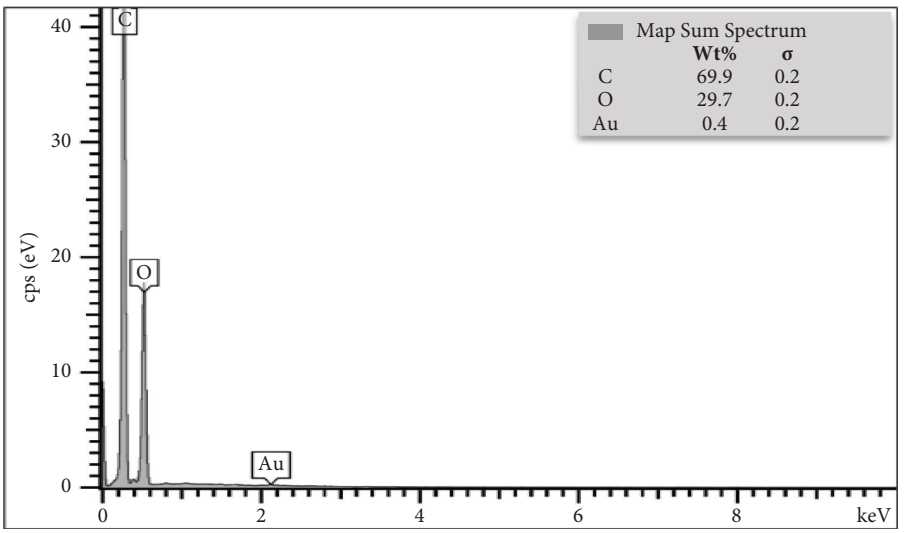

(c)

Figure 3: Continued.

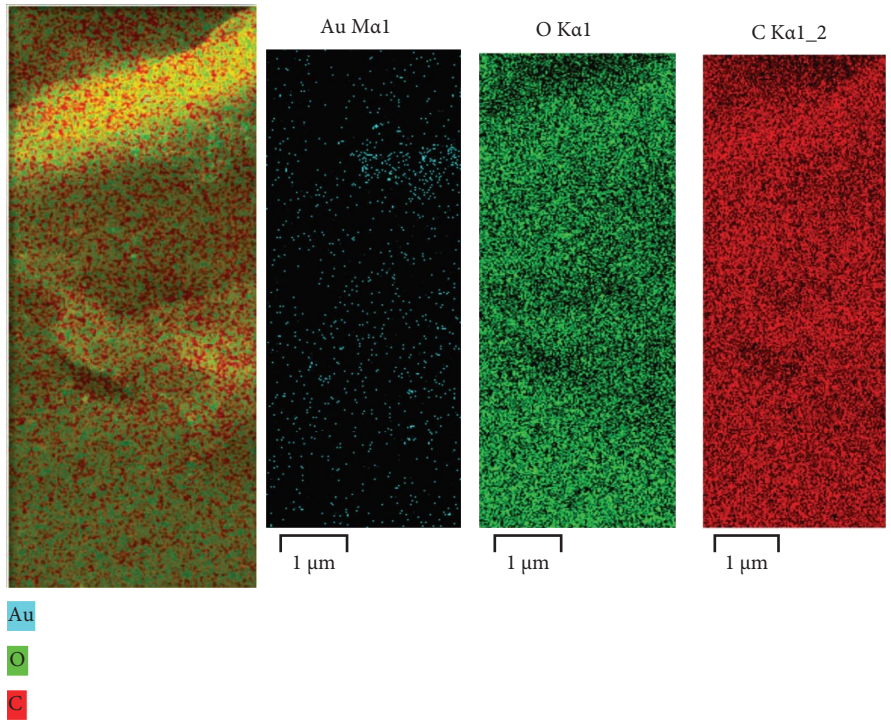

(d)

Figure 3: EDS-mapping of the GA before loading Au (III) (a, b) and after loading Au (III) (c, d) on it.

Table 2: CHN elemental analysis report of GA composition.

Composition	% C	% H	% N
GA	47.49	4.91	1.17

3.4.1. Effect of Interaction between pH and Adsorbent Mass. The percent of Au (III) adsorption decreased by increasing the pH up to 5, and it increased as the adsorbent amount increased from 7 to 35 mg (Figure 4(a)). Adsorption of the metal ions via the adsorbent surface depends on the solution pH which corresponds to the ionization form of the functional groups of adsorbent and the chemistry of metal in the solution, which influences the number of available active sites [49, 50]. An increase in the amount of adsorbent increases the active sites of the adsorbent surface; therefore, the number of ions that are adsorbed by the adsorbent increases [51, 52]. At low pH (<3), facile protonation of the adsorbent leads to its positive surface charge, and the dominant species of Au (III) anions is $AuCl_4^-$; therefore, this condition is desired for the Au (III) anions adsorption [39, 53–58].

At pH = 1, with a GA amount greater than 20 mg, the percentage of Au (III) adsorption reached 100%. The electrostatic attraction between Au (III) ions ($AuCl_4^-$) and the greater number of positive surface charges of the GA causes the Au (III) ions adsorbed by the GA to increase. At a pH above 1, with an increase in pH and a reduction in the GA amount, the percentage of adsorption reduces. At a high pH, some oxygenated functional groups are deprotonated, and $AuCl_4^-$ is hydrolyzed [39, 59, 60]. Therefore, the electrostatic repulsion between Au (III) ions and the small number of functional groups in GA increases, consequently, the Au (III) ions are repulsed by the GA surface, and the adsorption percentage decreases. Indeed, the pH and adsorbent mass interaction indicates that an increase in the adsorbent mass, accompanied by a simultaneous decrease in pH, increases the percentage of Au (III) adsorption by GA.

3.4.2. Effect of Interaction between pH and Au (III) Concentration. As is observed in Figure 4(b), the adsorption percentage of Au (III) increased significantly with a simultaneous decline in pH and Au (III) concentration. At a pH of 2.4 and a concentration less than 50 mg L^{-1}, the Au (III) adsorption percentage reached 100%. The number of active sites on the surface of the GA becomes less than the number of Au (III) molecules with an increase in Au (III) concentration in the solution [51, 61]. In consequence, the available sites on the surface of the GA are saturated very quickly, and more sites are required for the complete adsorption of the desired concentration; therefore, the amount of adsorption decreases with the increase in concentration.

3.4.3. Effect of Interaction between pH and Contact Time. Figure 4(c) shows that a decline in pH accompanied by an increase in contact time (10–50 min) leads to a significant increase in Au (III) adsorption percentage. In this condition, a reduction in pH leads to the positive surface charge of the GA and the rise of $AuCl_4^-$ species in the solution. Moreover,

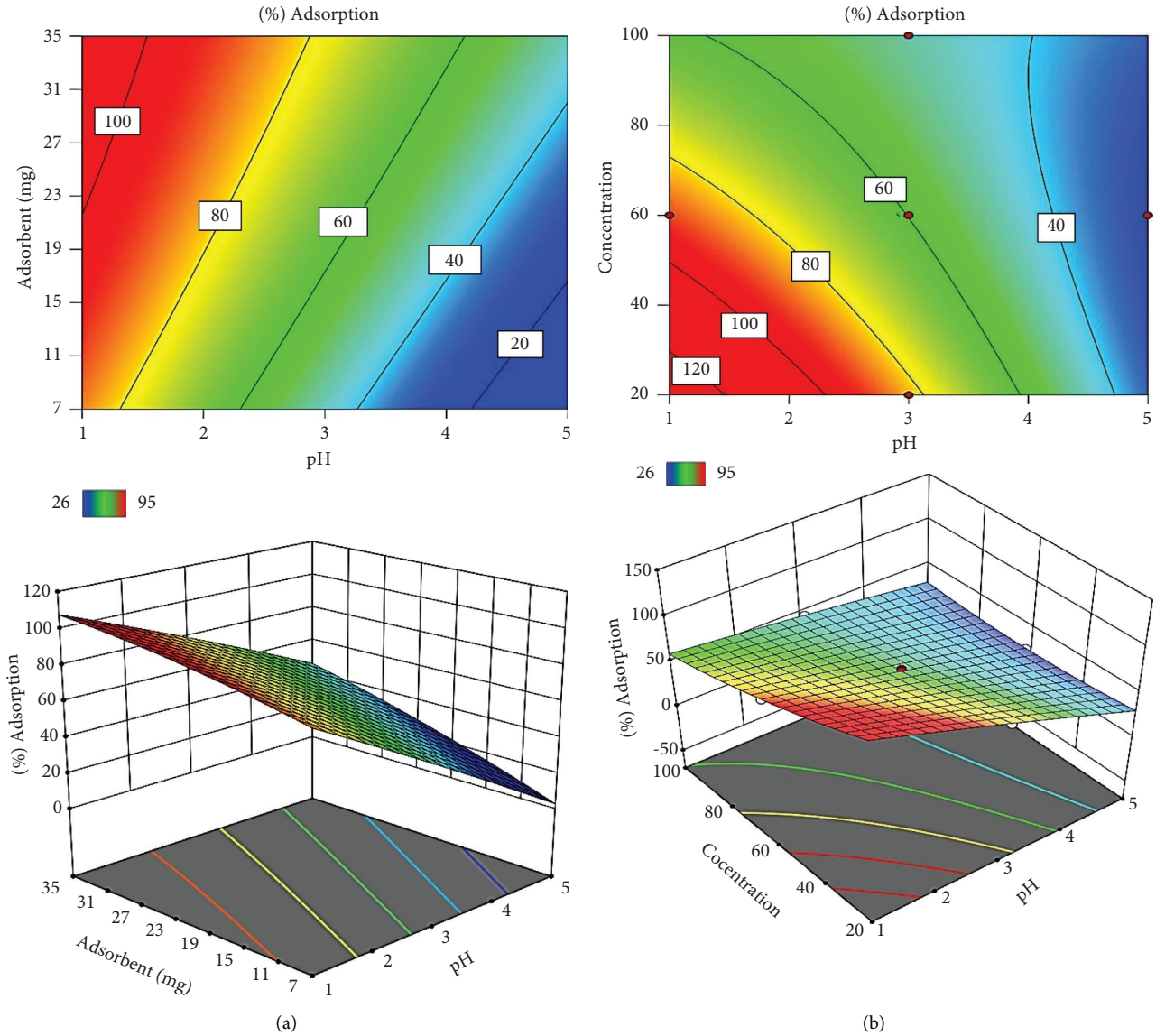

Figure 4: Continued.

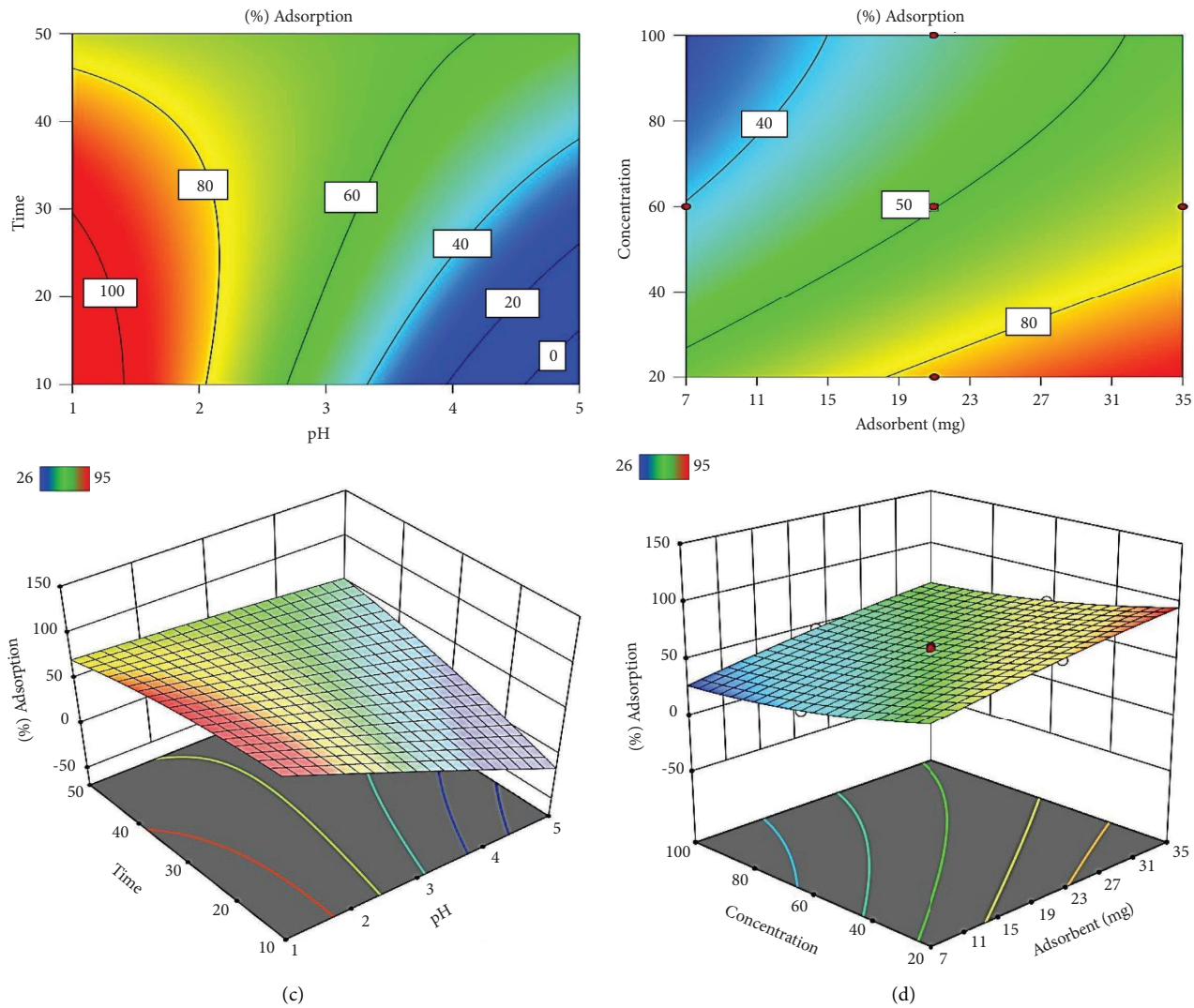

(c) (d)

Figure 4: Continued.

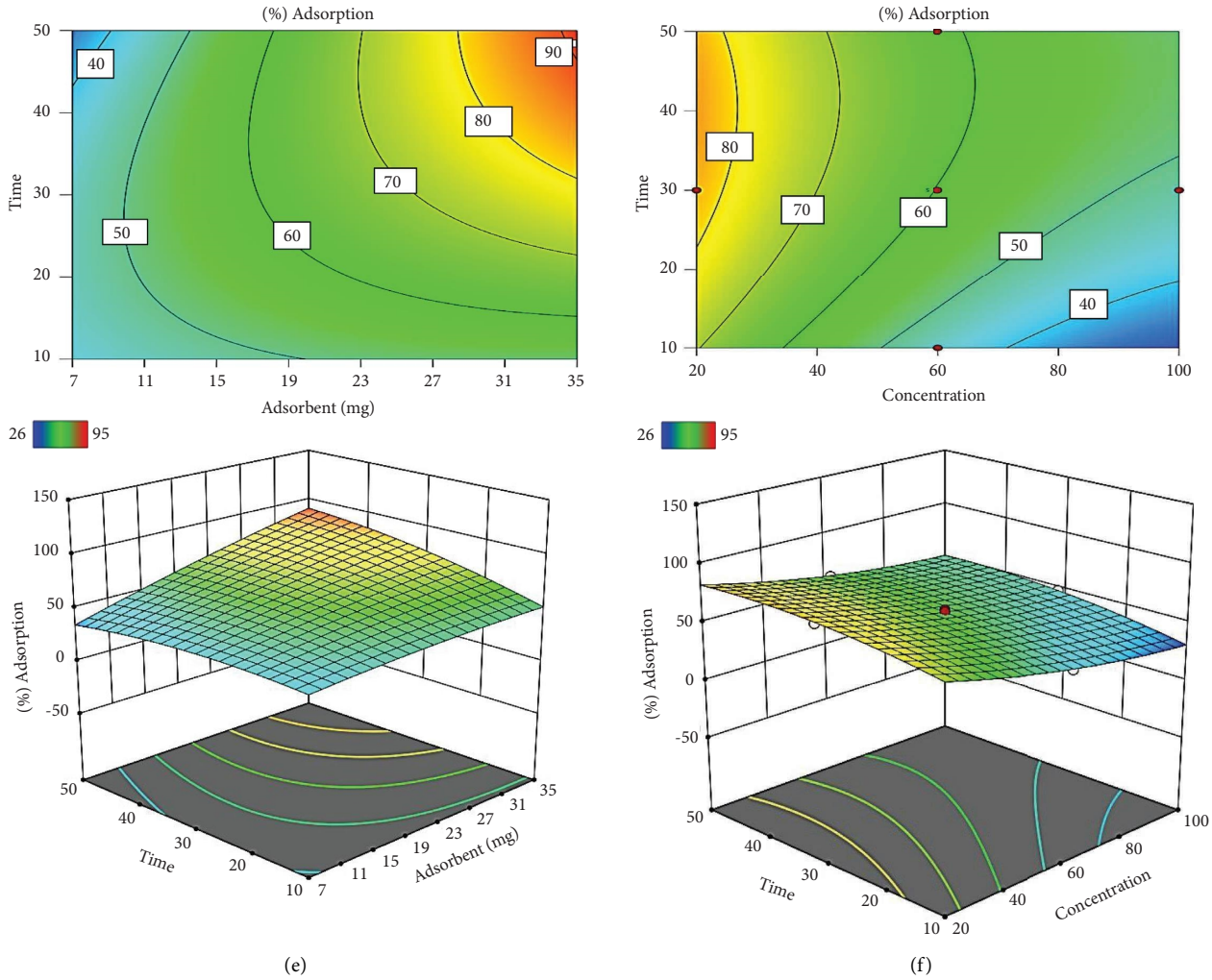

Figure 4: Contour plots and three-dimensional response surfaces of Au (III) adsorption via the GA representing interactions between different variables: (a) pH and adsorbent mass, (b) Au (III) concentration and pH, (c) contact time and pH, (d) Au (III) concentration and adsorbent mass, (e) contact time and adsorbent mass, and (f) contact time and Au (III) concentration.

by increasing the shaking time, Au (III) anions have adequate time to be adsorbed on the surface of the GA. The probable speed of the Au (III) adsorption process of GA is determined using contact time. As a result, the optimal time for the complete adsorption of Au (III) ions by the adsorbent is determined. At a pH between 1 and 2, less than 50 min of contact time is required for the adsorption percentage to reach 100%, which indicates the fast adsorption of gold ions on the GA surface.

3.4.4. Effect of Interaction between Adsorbent Mass and Au (III) Concentration. As shown in Figure 4(d), the Au (III) adsorption percentage increased by simultaneously increasing the mass of the GA and decreasing the Au (III) concentration. As the number of active sites on the surface of GA increased with the adsorbent portion, a reduction in the Au (III) concentration in the solution led to a smaller number of Au (III) molecules, and the adsorption rate of Au (III) ions was thus increased [51, 52].

3.4.5. Effect of Interaction between Adsorbent Mass and Contact Time. Figure 4(e) shows that the amount of Au (III) adsorption increased significantly with a simultaneous increase in the amount of GA and contact time. Due to increasing the amount of the GA, the active sites on its surface were increased. Moreover, by increasing the contact time, the active sites of the GA surface had more time to adsorb Au (III) ions [19, 51]. Consequently, the adsorption rate was 90% in a contact time of 50 min with the adsorbent mass of 35 mg.

3.4.6. Effect of Interaction between Au (III) Concentration and Contact Time. The interaction between Au (III) concentration and contact time is shown in Figure 4(f). By simultaneously reducing the concentration and raising the contact time, the Au (III) adsorption percentage was increased. These results show that GA had sufficient time to adsorb a few Au (III) ions. This can be attributed to the prolonged shaking time and low concentration of Au (III)

ions that led to an increase in the rate of Au (III) adsorption on the GA surface [19].

3.5. Mechanism of Au (III) Adsorption onto the GA Surface. Various mechanisms including electrostatic interaction and reduction have been suggested for gold adsorption by biosorbents containing hydroxyl groups [2, 9, 14]. Acidic medium leads to protonation of the surface of biosorbents with phenolic compounds and their positive charge. As aforementioned, the dominant form of Au (III) ions in the acidic medium is the chloro complex anion [39, 53–58].

Accordingly, the positive surface charge of GA attracts gold anionic species via electrostatic attraction. Hence, the electrostatic attraction mechanism is considered to be the main factor responsible for Au (III) adsorption by the GA surface.

Gold has a high reduction potential and acts as an oxidizing species. On the contrary, phenolic hydroxyl groups are very sensitive to oxidation [2, 9, 14, 62]. Thus, Au (III) anionic species adsorbed on the GA by electrostatic interaction are reduced to Au (0) by the hydroxyl phenolic groups of the GA. Therefore, it is reasonable to suggest the combination of electrostatic interactions and reduction as the mechanisms of Au (III) adsorption on the GA surface (Figure 5).

3.6. Adsorption Equilibrium Isotherms. The isotherm inquiry of Au (III) adsorbed on the GA was defined by Freundlich, Temkin, Dubinin–Radushkevich, and Langmuir isotherms. The sorption isotherm illustrates the interaction between the adsorbent and the adsorbed component and is used to define the adsorption capacity of the adsorbent and optimize the adsorption process [63–65]. The Langmuir isotherm illustrates a monolayer adsorption. In this model, all adsorption sites have the same energy and enthalpy, and there is no interaction between the adsorbed molecules and the absorbent surface [66, 67]. Freundlich isotherm exemplifies multilayer sorption and heterogeneous surface adsorption underneath diverse nonideal circumstances. The Temkin model expresses a situation in which the adsorption heat declines linearly with an increase in the capacity of adsorption. The mechanism of adsorption via a Gaussian distribution of energy on a heterogeneous surface is described by Dubinin–Radushkevich [38, 68–71]. Table S4 shows the parameters of isotherm models. Adsorption isotherms were performed using the optimum values of pH = 2, contact time = 30 min, and adsorbent amount = 23 mg to determine the GA adsorption capacity.

The most appropriate isotherm for adsorption studies was selected by comparing the correlation coefficients (R^2) of the isotherm equations [64]. If R^2 for each model is closer to 1, then the model is more appropriate. As shown in Table S4, the Freundlich model is more suitable than other models, because its R^2 is closest to 1 and is greater than the R^2 values of other models. The maximum adsorption capacity of the GA for Au (III) adsorption was 315.450 mg g^{-1}. Table 3 shows the adsorption capacities of Au (III) for several adsorbents. It can be seen that GA has a high affinity with Au

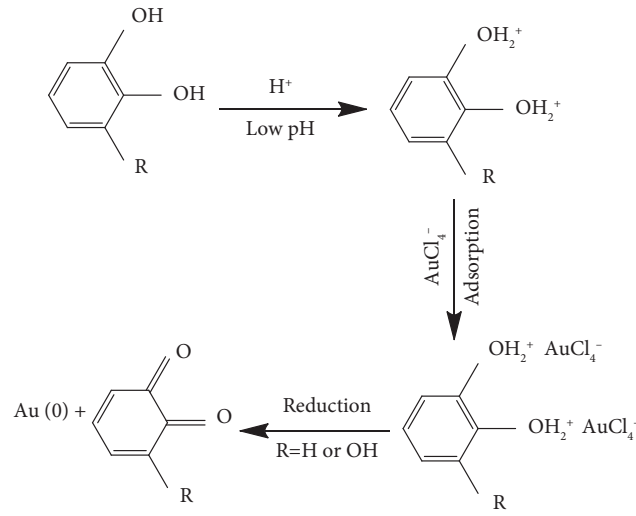

Figure 5: Scheme of the possible mechanism of gold adsorption by the GA.

(III) ions due to the presence of a large number of phenolic hydroxyl groups on its porous surface.

The verification of experimental data with the Freundlich model shows the heterogeneity of the GA. In addition, the results exhibited that the gold molecules formed a multilayer coating on the GA surface. The value of $(1/n)$ less than 1 implies a desirable adsorption of Au (III) onto GA. The dimensionless parameter (R_L) indicates the nature of adsorption with $R_L = 0$ indicating the irreversible adsorption process, $R_L > 1$ showing an undesirable adsorption process, $0 < R_L < 1$ demonstrating a desirable adsorption process, and $RL = 1$ representing a linear process [17, 55, 64, 71, 80, 81]. The obtained value for R_L (0.421–0.814) was less than one, indicating that the adsorption process was desirable.

3.7. Kinetic Studies and Activation Energy. Two important factors in the adsorption process are rate constants and order of reaction. The kinetic investigation of Au (III) adsorbed on the GA was determined by the pseudo-first-order (PFO), pseudo-second-order (PSO), Elovich, and intraparticle diffusion models.

In the pseudo-first-order model, diffusion happens in a single layer where the change in adsorption with time is commensurate with the absorbent surface of unoccupied sites. The pseudo-second-order model shows that chemical interactions are the rate-controlling stage in the adsorption process, where the rate of occupancy of adsorption sites is proportional to the number of occupied ones. The chemical interactions include forces via the sharing or swap of electrons between the adsorbed component and the adsorbent [66, 70]. Determining the effectual stages on the rate of the adsorption process and the rate control stage is accomplished by intraparticle diffusion [70]. Elovich's model depicts chemisorption [64].

The kinetic model parameters are shown in Table S5. The most suitable model was selected according to R^2. The R^2 quantity of the pseudo-second-order model is closest to 1 and is larger than the R^2 quantity of other models. Therefore,

Table 3: Comparison of adsorption capacities, time required, and temperature to reach the equilibrium of several adsorbents for Au (III).

Adsorbents	Q_m (mg g^{-1})	Isotherm	Kinetic	pH	T (K)	Time (h)	Reference
DACS-TA	298.5	Langmuir	PSO	2	333	22	[53]
Asn@SBA-15	307	Langmuir	PSO	2.09	303	2.5	[55]
UHMWPE-g-PAO	220	Freundlich	—	3	298	—	[60]
PANF-ATL	130.58	Langmuir	PSO	0.1 M HCl	298	4	[63]
CFP-g-PHCTMA	137.6	—	PSO	0.1 M HCl	298	3	[72]
AIAC	191.92	Langmuir	PSO	1	298	24	[73]
3, 4-DHB-MCM-41	290	—	—	5	298	—	[74]
D301-g-THIOPGMA	300.4	Langmuir	PFO	2	298	5	[75]
D301-g-EDAPGMA	274.7	Langmuir	PFO	2	298	5	[75]
Graphene oxide	108.342	Langmuir	PSO	6	298	6	[76]
PPF resin	506	—	—	0.58 M HCl	303	24	[77]
GO	159.34	Langmuir	PFO and PSO	11	298	1	[78]
GO	171.23	Langmuir	—	11	308	—	[78]
Au-C-PTS	140.54	Langmuir	PSO	5	303	3	[79]
GA	315.450	Freundlich	PSO	2	303	0.5	This work

the pseudo-second-order model is more appropriate to express the kinetic of the adsorption process of Au (III) on the GA surface. Furthermore, the values of q_e obtained (q_e (exp)) and calculated (q_e (calc)) by the pseudo-second-order model are very close to each other, indicating that this model is very suitable for representing the experimental data. These results show chemical interactions between gold molecules and the GA surface. Table 3 shows the time required to reach the equilibrium for the GA compared to several adsorbents. It can be seen that gold adsorption on the GA reaches the equilibrium state in a much shorter time than other adsorbents, signifying the fast adsorption of gold by the GA.

By using kinetic data at diverse temperatures, the activation energy (E_a) for the gold adsorption process was calculated. Activation energy is the least energy needed for reacting adsorbed molecules with functional groups of adsorbent. The negative E_a means that the adsorption process is carried out at a low temperature and its nature is exothermic. Contrarily, the positive E_a indicates that the adsorption process is accomplished at a high temperature and the process needs energy and its nature is endothermic [82–84]. E_a is measured using the following Arrhenius equation:

$$\mathrm{Ln}\, K = -\frac{E_a}{\mathrm{RT}} + \mathrm{Ln}\, A, \tag{2}$$

where A is the Arrhenius factor, K is the rate constant, T is the temperature, and R is the universal gas constant. The Ln K versus 1/T plot provides a straight line and E_a is the slope of that line. E_a for the gold adsorption process was 30.178 kJ·mol^{-1} (Figure 6). The type of adsorption (physisorption or chemisorption) can be determined by the amount of activation energy. Physisorption needs an activation energy of less than 40 kJ·mol^{-1}. Physisorption is commonly reversible [84]. Accordingly, the gold adsorption process on the GA surface might be physisorption and reversible.

3.8. Thermodynamic Studies. The influence of temperature on the adsorption of Au (III) at different temperatures was studied and the thermodynamic factors entropy (ΔS^0), enthalpy (ΔH^0), and Gibbs free energy (ΔG^0) were computed using the following equations [79, 85–88]:

$$\begin{aligned} 4)\ K_d &= \frac{C_{\mathrm{ads}}}{C_e}, \\ 5)\ \mathrm{Ln}K_d &= -\frac{\Delta H^0}{\mathrm{RT}} + \frac{\Delta S^0}{R}, \\ 6)\ \Delta G^0 &= -\mathrm{RTLn}\, K_d, \end{aligned} \tag{3}$$

where K_d is the adsorption distribution coefficient, C_{ads} is the amount of Au (III) adsorbed by the GA at equilibrium (mg L^{-1}), C_e is the amount of Au (III) residual in the solution at equilibrium (mg L^{-1}), T (K°) is the solution temperature, and R (8.314 J·mol^{-1} K^{-1}) is the universal gas constant. The amount of ΔS^0 and ΔH^0 was measured from the slope and intercept of the Ln K_d plot versus (1/T).

An increase in the temperature causes changes in the adsorption process by increasing the diffusion of the adsorbate molecules in the outer border layer and the internal pores of the absorbent particles and changing the adsorbent equilibrium capacity for a peculiar adsorbate [63]. As seen in Table S6, the percentage of Au (III) adsorption by the GA increases with rising temperature, and the $\Delta H^0 > 0$ verifies the endothermic nature of the adsorption process. The $\Delta G^0 < 0$ demonstrates that the adsorption process of Au (III) was spontaneous. $\Delta S^0 > 0$ depicts a rise in disorder at the solid-liquid interface upon adsorption. Table 3 depicts the temperature required to reach the equilibrium for the GA compared to several adsorbents. As can be seen, gold adsorption on the GA reaches the equilibrium at 303 K.

3.9. Effect of Competing Metals in the Real Sample (Waste PCB) on Gold Adsorption. There are several metals accompanying gold in PCBs. The presence of these competing metals may affect the adsorption of gold by the GA. Therefore, it is mandatory to examine the selectivity of the GA for the gold. GA application for gold recovery from the PCB matrix was investigated using competing metals with different concentrations (pH = 2, adsorbent mass = 23 mg,

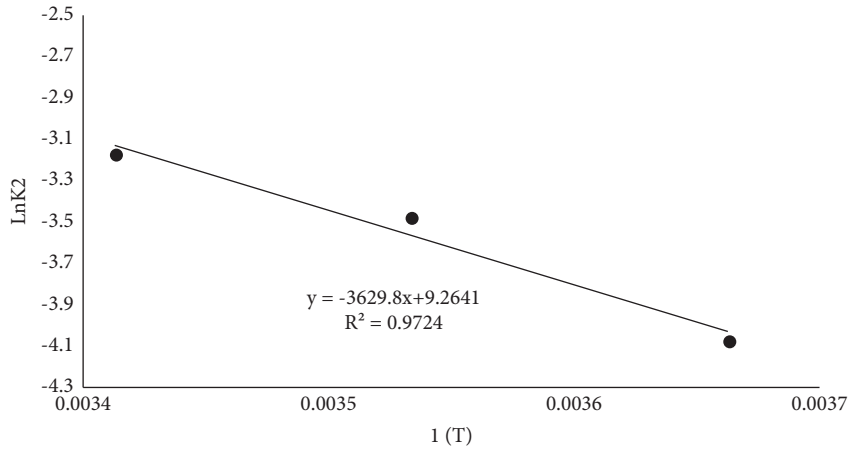

Figure 6: Plot of ln k_2 vs. 1 (T) (Arrhenius plot).

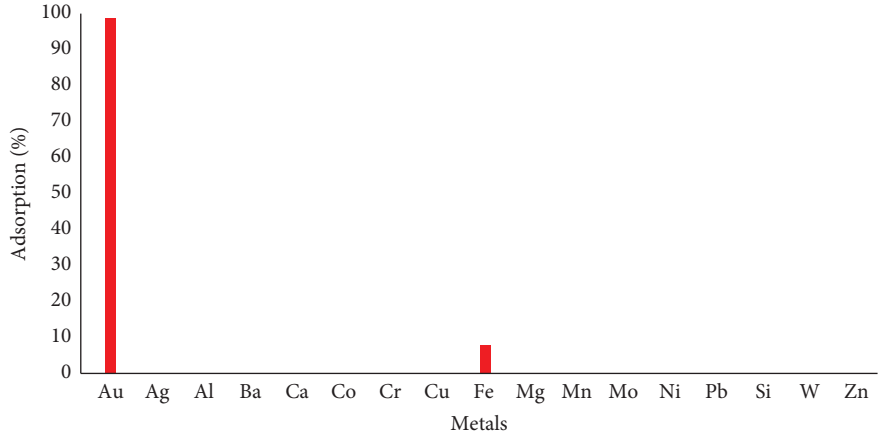

Figure 7: Effect of competing metals in the waste PCB on Au (III) adsorption. The initial concentration of metals in the solution at pH = 2 (Au = 30.12, Ag = 6, Al = 8423, Ba = 133, Ca = 1160, Co = 2, Cr = 59, Cu = 8196, Fe = 744, Mg = 71, Mn = 13.6, Mo = 1, Ni = 176, Pb = 16.3, Si = 7, W = 0.3, and Zn = 40 mg L^{-1}), volume of solution = 5 mL, adsorbent mass = 23 mg, temperature = 303 K, and contact time = 30 min.

Table 4: Comparison of adsorbent mass and the number of competing metals of several adsorbents for gold adsorption.

Adsorbents	Adsorbent mass (mg)	Competing metals	Reference
DACS-TA	50	Cr, Fe, Al, Sb, Cu, Ni, and Zn	[53]
AS–5BA	50	Fe, Cu, and Zn	[57]
BHJC	20	Hg, Cu, Pb, Ni, Zn, Cd, Cr, and Co	[58]
PANF-ATL	15	Ni, Cd, Cu, Zn, and Pb	[63]
DTGA–XAD16	30	Cr, Ni, Ba, Sn, Fe, Se, Zn, Pb, Cu, As, and Y	[68]
D301-g-EDAPGMA	10	Cu and Zn	[75]
Au-C-PTS	100	Hg, Cu, Cd, and Fe	[79]
GA	23	Ag, Al, Si, Zn, Pb, Ba, Ni, Ca, Mo, Co, Cr, Mn, Cu, Mg, Fe, and W	This work

temperature = 303 K, and contact time = 30 min), and the outcomes are shown in Figure 7. As shown in Figure 7, GA has an excellent selectivity for gold adsorption as its positive surface attracts negatively charged gold anions by electrostatic attraction. GA's affinity to adsorb iron was negligible and the adsorption of other metals on the GA surface was zero.

Despite the anionic form of gold, the base metal ions exist mainly in the cationic or neutral form in an acidic medium; and hence, they are not adsorbed on GA due to the electrostatic repulsion between them and the positive surface charge of GA [39, 59, 62]. Table 4 shows the adsorbent mass and the number of competing metals of several adsorbents for gold adsorption. Compared to other adsorbents, a small amount of the GA adsorbed gold from a larger number of metals present in the real sample.

3.10. Reusability of GA. Adsorbent regeneration is important because of economic and resource considerations. The adsorption efficiency of GA recycled in three successive cycles

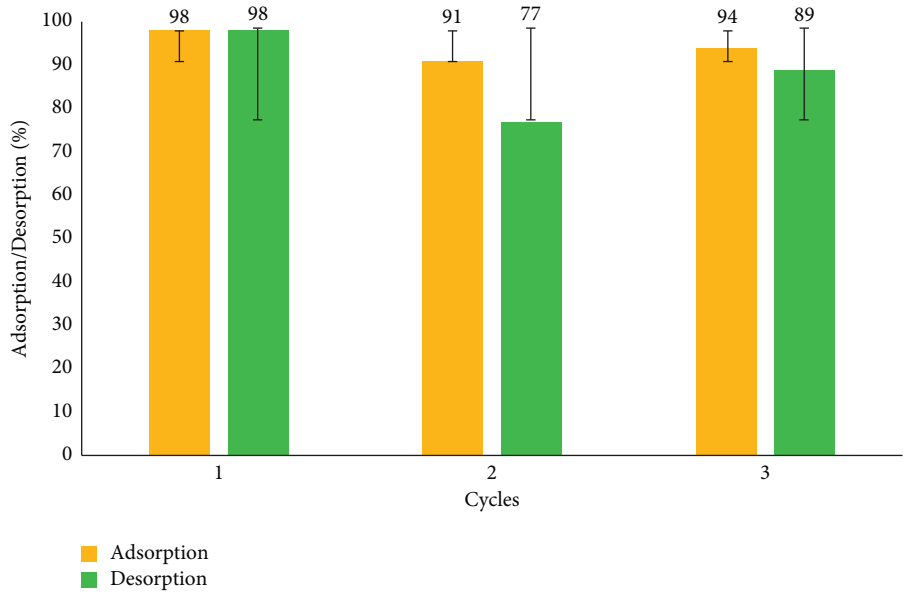

Figure 8: Reusability of the GA. Adsorption conditions: Au (III) concentration = 32 mg L^{-1}, GA mass = 23 mg, pH = 2, and contact time = 30 min. Desorption conditions: elution agent = solution of thiourea (0.5 M) in HCl (2 M) and shaking time = 4 h.

was evaluated, and experimental examinations were performed using 32 mg L^{-1} of Au (III) and 23 mg of GA at pH = 2, with a contact time of 30 min. Elution of gold loaded on the GA surface was accomplished using thiourea (0.5 M) in HCl (2 M) by shaking for 4 hours. The GA showed over 90% adsorption for the three cycles (Figure 8). Hence, the GA could be a reusable and cost-effective adsorbent. The rapid elution of gold loaded on the GA surface implies that gold adsorption on the GA surface can be physical and reversible.

4. Conclusion

In this research, the GA was utilized for the fast and selective recovery of Au (III) from waste PCBs. In optimum conditions of pH = 2, adsorbent mass = 23 mg, Au (III) concentration = 32 mg L^{-1}, and contact time = 30 min, experimental adsorption percentage was 97%. The highest capacity of the GA to adsorb Au (III) was 315. 450 mg g^{-1}. Freundlich ($R^2 = 0.952$) and pseudo-second-order ($R^2 = 0.998$) models expressed the isotherm and kinetic of Au (III) adsorption onto the GA. The thermodynamics of Au (III) adsorption by the GA was an endothermic ($\Delta H^\circ > 0$), facile ($\Delta S^\circ > 0$), and spontaneous ($\Delta G^\circ < 0$) process. The adsorption mechanism could include several reactions of electrostatic interaction and reductive adsorption. GA adsorbed gold with the highest adsorption percentage (97%) along with an excellent selectivity from competing metals (Ag, Al, Si, Zn, Pb, Ba, Ni, Ca, Mo, Co, Cr, Mn, Cu, Mg, Fe, and W) in waste PCB. The outcomes of this study suggest the use of the GA with low cost, high effectiveness, and selectivity to recover gold from secondary sources such as waste PCBs.

Data Availability

Data supporting the results of this article are presented as supplementary materials.

Disclosure

This article was extracted from a Ph.D. thesis.

Conflicts of Interest

The authors declare that they have no conflicts of interest.

Acknowledgments

We would like to thank Dr. Abdolhadi Farrokhnia for helping us. Also, we thank everyone who helped us in this work. This work was supported by Shahrekord University.

Supplementary Materials

Tables S1–S3 show the CCD experimental design and Tables S4–S6 show the isotherm, kinetic, and thermodynamic parameters. (*Supplementary Materials*)

References

[1] H. Y. Kang and J. M. Schoenung, "Electronic waste recycling: a review of U.S. infrastructure and technology options," *Resources, Conservation and Recycling*, vol. 45, no. 4, pp. 368–400, 2005.

[2] T. Ogata and Y. Nakano, "Mechanisms of gold recovery from aqueous solutions using a novel tannin gel adsorbent synthesized from natural condensed tannin," *Water Research*, vol. 39, no. 18, pp. 4281–4286, 2005.

[3] Q. Yi, R. Fan, F. Xie, H. Min, Q. Zhang, and Z. Luo, "Selective recovery of Au(III) and Pd(II) from waste PCBs using ethylenediamine modified persimmon tannin adsorbent," *Procedia Environmental Sciences*, vol. 31, pp. 185–194, 2016.

[4] F. Xie, Z. Fan, Q. Zhang, and Z. Luo, "Selective adsorption of $Au^{3+}$from aqueous solutions using persimmon powder-formaldehyde resin," *Journal of Applied Polymer Science*, vol. 130, pp. 3937–3946, 2013.

[5] R. Fan, H. Min, X. Hong et al., "Plant tannin immobilized Fe3O4@SiO2 microspheres: a novel and green magnetic biosorbent with superior adsorption capacities for gold and palladium," *Journal of Hazardous Materials*, vol. 364, pp. 780–790, 2019.

[6] A. Golnaraghi Ghomi, N. Asasian-Kolur, S. Sharifian, and A. Golnaraghi, "Biosorpion for sustainable recovery of precious metals from wastewater," *Journal of Environmental Chemical Engineering*, vol. 8, no. 4, Article ID 103996, 2020.

[7] F. B. Biswas, I. M. M. Rahman, K. Nakakubo et al., "Comparative evaluation of dithiocarbamate-modified cellulose and commercial resins for recovery of precious metals from aqueous matrices," *Journal of Hazardous Materials*, vol. 418, Article ID 126308, 2021.

[8] M. Gurung, B. B. Adhikari, H. Kawakita, K. Ohto, K. Inoue, and S. Alam, "Recovery of Au(III) by using low cost adsorbent prepared from persimmon tannin extract," *Chemical Engineering Journal*, vol. 174, no. 2-3, pp. 556–563, 2011.

[9] T. Ogata, Y. H. Kim, and Y. Nakano, "Selective recovery process for gold utilizing a functional gel derived from natural condensed tannin," *Journal of Chemical Engineering of Japan*, vol. 40, no. 3, pp. 270–274, 2007.

[10] D. Parajuli, H. Kawakita, K. Inoue, K. Ohto, and K. Kajiyama, "Persimmon peel gel for the selective recovery of gold," *Hydrometallurgy*, vol. 87, no. 3-4, pp. 133–139, 2007.

[11] H. Kawakita, R. Yamauchi, D. Parajuli, K. Ohto, H. Harada, and K. Inoue, "Recovery of gold from hydrochloric acid by means of selective coagulation with persimmon extract," *Separation Science and Technology*, vol. 43, no. 9-10, pp. 2375–2385, 2008.

[12] D. Parajuli, H. Kawakita, K. Kajiyama, K. Ohto, H. Harada, and K. Inoue, "Recovery of gold from hydrochloric acid by using lemon peel gel," *Separation Science and Technology*, vol. 43, no. 9-10, pp. 2363–2374, 2008.

[13] D. Parajuli, C. R. Adhikari, H. Kawakita, S. Yamada, K. Ohto, and K. Inoue, "Chestnut pellicle for the recovery of gold," *Bioresource Technology*, vol. 100, no. 2, pp. 1000–1002, 2009.

[14] H. Kawakita, M. Abe, J. I. Inoue, K. Ohto, H. Harada, and K. Inoue, "Selective gold recovery using orange waste," *Separation Science and Technology*, vol. 44, no. 12, pp. 2797–2805, 2009.

[15] B. Pangeni, H. Paudyal, K. Inoue, H. Kawakita, K. Ohto, and S. Alam, "Selective recovery of gold(III) using cotton cellulose treated with concentrated sulfuric acid," *Cellulose*, vol. 19, no. 2, pp. 381–391, 2012.

[16] H. Zheng and L. Wang, "Banana peel carbon that containing functional groups applied to the selective adsorption of Au(III) from waste printed circuit boards," *Soft Nanoscience Letters*, vol. 3, no. 2, pp. 29–36, 2013.

[17] B. C. Choudhary, D. Paul, A. U. Borse, and D. J. Garole, "Surface functionalized biomass for adsorption and recovery of gold from electronic scrap and refinery wastewater," *Separation and Purification Technology*, vol. 195, pp. 260–270, 2018.

[18] H. A. M. Bacelo, S. C. R. Santos, and C. M. S. Botelho, "Tannin-based biosorbents for environmental applications – a review," *Chemical Engineering Journal*, vol. 303, pp. 575–587, 2016.

[19] P. Arabkhani, H. Javadian, A. Asfaram, and S. N. Hosseini, "A reusable mesoporous adsorbent for efficient treatment of hazardous triphenylmethane dye wastewater: RSM-CCD optimization and rapid microwave-assisted regeneration," *Scientific Reports*, vol. 11, pp. 22751–22818, 2021.

[20] M. Foschi, P. Capasso, M. A. Maggi, F. Ruggieri, and G. Fioravanti, "Experimental design and response surface methodology applied to graphene oxide reduction for adsorption of triazine herbicides," *ACS Omega*, vol. 6, no. 26, pp. 16943–16954, 2021.

[21] R. Singh and R. Bhateria, "Optimization and experimental design of the Pb^{2+} adsorption process on a nano-Fe_3O_4-based adsorbent using the response surface methodology," *ACS Omega*, vol. 5, no. 43, pp. 28305–28318, 2020.

[22] A. R. Bagheri, M. Ghaedi, A. Asfaram, A. A. Bazrafshan, and R. Jannesar, "Comparative study on ultrasonic assisted adsorption of dyes from single system onto Fe3O4 magnetite nanoparticles loaded on activated carbon: experimental design methodology," *Ultrasonics Sonochemistry*, vol. 34, pp. 294–304, 2017.

[23] A. R. Bagheri, M. Ghaedi, A. Asfaram, R. Jannesar, and A. Goudarzi, "Design and construction of nanoscale material for ultrasonic assisted adsorption of dyes: application of derivative spectrophotometry and experimental design methodology," *Ultrasonics Sonochemistry*, vol. 35, pp. 112–123, 2017.

[24] E. Sharifpour, H. Haddadi, M. Ghaedi, A. Asfaram, and S. Wang, "Simultaneous and rapid dye removal in the presence of ultrasound waves and a nano structured material: experimental design methodology, equilibrium and kinetics," *RSC Advances*, vol. 6, no. 70, pp. 66311–66319, 2016.

[25] F. Nasiri Azad, M. Ghaedi, K. Dashtian, S. Hajati, A. Goudarzi, and M. Jamshidi, "Enhanced simultaneous removal of malachite green and safranin O by ZnO nanorod-loaded activated carbon: modeling, optimization and adsorption isotherms," *New Journal of Chemistry*, vol. 39, no. 10, pp. 7998–8005, 2015.

[26] A. Tadjarodi, S. Moazen Ferdowsi, R. Zare-Dorabei, and A. Barzin, "Highly efficient ultrasonic-assisted removal of Hg(II) ions on graphene oxide modified with 2-pyridinecarboxaldehyde thiosemicarbazone: adsorption isotherms and kinetics studies," *Ultrasonics Sonochemistry*, vol. 33, pp. 118–128, 2016.

[27] M. S. Tehrani and R. Zare-Dorabei, "Competitive removal of hazardous dyes from aqueous solution by MIL-68(Al): derivative spectrophotometric method and response surface methodology approach," *MolmolSpectrochimica Acta Part A: Molecular and Biomolecular Spectroscopy*, vol. 160, pp. 8–18, 2016.

[28] E. Sharifpour, H. Haddadi, M. Ghaedi, K. Dashtian, and A. Asfaram, "Synthesis of antimicrobial cationic amphiphile functionalized mesocellular silica foam prepared on hard template/support activated carbon for enhanced simultaneous removal of Cu(II) and Zn(II) ions," *Journal of Environmental Chemical Engineering*, vol. 6, no. 4, pp. 4864–4877, 2018.

[29] F. Zandi-Darehgharibi, H. Haddadi, M. Rafieian-Kopaei, and A. A. Fallah, "Effects of pistachio green hull crude extract and its polyphenol fraction on oxidative stability of sunflower oil during accelerated storage," *Biomass Conversion and Biorefinery*, pp. 1–8, 2021.

[30] A. Hubau, A. Chagnes, M. Minier, S. Touzé, S. Chapron, and A. G. Guezennec, "Recycling-oriented methodology to sample and characterize the metal composition of waste Printed Circuit Boards," *Waste Management*, vol. 91, pp. 62–71, 2019.

[31] L. Abed and N. Belattar, "Polyphenols content, chelating propertiesand adsorption isotherms and kinetics of redand yellow pomegranate peels (punica granatum L.)Towards lead

(II)," *Polish Journal of Environmental Studies*, vol. 31, pp. 5765–5779, 2022.

[32] H. Haddadi, N. Alizadeh, and M. Shamsipur, "Stoichiometric and free radical-scavenging kinetic studies of extractable polyphenols from pomegranate husk and pistachio hull," *Journal of the Iranian Chemical Society*, vol. 8, no. 3, pp. 694–707, 2011.

[33] B. Singh, J. P. Singh, A. Kaur, and N. Singh, "Antimicrobial potential of pomegranate peel: a review," *International Journal of Food Science and Technology*, vol. 54, pp. 959–965, 2019.

[34] A. A. Saparbekova, G. O. Kantureyeva, D. E. Kudasova, Z. K. Konarbayeva, and A. S. Latif, "Potential of phenolic compounds from pomegranate (Punica granatum L.) by-product with significant antioxidant and therapeutic effects: a narrative review," *Saudi Journal of Biological Sciences*, vol. 30, no. 2, Article ID 103553, 2023.

[35] K. Kaderides, I. Mourtzinos, and A. M. Goula, "Stability of pomegranate peel polyphenols encapsulated in orange juice industry by-product and their incorporation in cookies," *Food Chemistry*, vol. 310, Article ID 125849, 2020.

[36] S. Smaoui, H. B. Hlima, A. C. Mtibaa et al., "Pomegranate peel as phenolic compounds source: advanced analytical strategies and practical use in meat products," *Meat Science*, vol. 158, Article ID 107914, 2019.

[37] Y. Mo, J. Ma, W. Gao et al., "Pomegranate peel as a source of bioactive compounds: a mini review on their physiological functions," *Frontiers in Nutrition*, vol. 9, Article ID 887113, 2022.

[38] A. Asfaram, M. Ghaedi, M. H. A. Azqhandi, A. Goudarzi, and M. Dastkhoon, "Statistical experimental design, least squares-support vector machine (LS-SVM) and artificial neural network (ANN) methods for modeling the facilitated adsorption of methylene blue dye," *RSC Advances*, vol. 6, no. 46, pp. 40502–40516, 2016.

[39] F. Liu, L. Zhou, L. Tao, L. Qian, G. Yu, and S. Deng, "Adsorption behavior and mechanism of Au(III) on caffeic acid functionalized viscose staple fibers," *Chemosphere*, vol. 253, Article ID 126704, 2020.

[40] P. B. Raja, A. A. Rahim, A. K. Qureshi, and K. Awang, "Green synthesis of silver nanoparticles using tannins," *Materials Science-Poland*, vol. 32, no. 3, pp. 408–413, 2014.

[41] F. G. Mendonça, T. G. Silva, G. M. do Nascimento, H. O. Stumpf, R. V. Mambrini, and W. D. do Pim, "Human hair as adsorbent of palladium(II) in solution: a precursor of well-dispersed size-controlled Pd nanoparticles," *Journal of the Brazilian Chemical Society*, vol. 30, pp. 736–743, 2018.

[42] I. A. Şengil and M. Özacar, "Biosorption of Cu(II) from aqueous solutions by mimosa tannin gel," *Journal of Hazardous Materials*, vol. 157, no. 2-3, pp. 277–285, 2008.

[43] Y. Boutaleb, R. Zerdoum, N. Bensid, R. A. Abumousa, Z. Hattab, and M. Bououdina, "Adsorption of Cr(VI) by mesoporous pomegranate peel biowaste from synthetic wastewater under dynamic mode," *Water*, vol. 14, no. 23, p. 3885, 2022.

[44] I. Akkari, Z. Graba, N. Bezzi, F. A. Merzeg, N. Bait, and A. Ferhati, "Raw pomegranate peel as promise efficient biosorbent for the removal of Basic Red 46 dye: equilibrium, kinetic, and thermodynamic studies," *Biomass Conversion and Biorefinery*, vol. 13, no. 9, pp. 8047–8060, 2023.

[45] Ç.Ö. Ay, A. S. Özcan, Y. Erdoğan, and A. Özcan, "Characterization of Punica granatum L. peels and quantitatively determination of its biosorption behavior towards lead(II) ions and Acid Blue 40," *Colloids and Surfaces B: Biointerfaces*, vol. 100, pp. 197–204, 2012.

[46] S. Ben-Ali, I. Jaouali, S. Souissi-Najar, and A. Ouederni, "Characterization and adsorption capacity of raw pomegranate peel biosorbent for copper removal," *Journal of Cleaner Production*, vol. 142, pp. 3809–3821, 2017.

[47] S. Ben-Ali, "Application of raw and modified pomegranate peel for wastewater treatment: a literature overview and analysis," *International Journal of Chemical Engineering*, vol. 2021, Article ID 8840907, 19 pages, 2021.

[48] A. Hashem, C. O. Aniagor, M. Fikry, G. M. Taha, and S. M. Badawy, "Characterization and adsorption of raw pomegranate peel powder for lead (II) ions removal," *Journal of Material Cycles and Waste Management*, vol. 25, no. 4, pp. 2087–2100, 2023.

[49] A. F. Ngomsik, A. Bee, J. M. Siaugue, D. Talbot, V. Cabuil, and G. Cote, "Co(II) removal by magnetic alginate beads containing Cyanex 272®," *Journal of Hazardous Materials*, vol. 166, no. 2-3, pp. 1043–1049, 2009.

[50] H. I. Adegoke, F. AmooAdekola, O. S. Fatoki, and B. J. Ximba, "Adsorption of Cr (VI) on synthetic hematite (α-Fe2O3) nanoparticles of different morphologies," *Korean Journal of Chemical Engineering*, vol. 31, no. 1, pp. 142–154, 2014.

[51] P. Arabkhani and A. Asfaram, "Development of a novel three-dimensional magnetic polymer aerogel as an efficient adsorbent for malachite green removal," *Journal of Hazardous Materials*, vol. 384, Article ID 121394, 2020.

[52] R. Panda, O. S. Dinkar, M. K. Jha, and D. D. Pathak, "Novel approach for selective recovery of gold, copper, and iron as marketable product from industrial effluent," *Gold Bulletin*, vol. 53, no. 1, pp. 11–18, 2020.

[53] F. Liu, G. Peng, T. Li, G. Yu, and S. Deng, "Au(III) adsorption and reduction to gold particles on cost-effective tannin acid immobilized dialdehyde corn starch," *Chemical Engineering Journal*, vol. 370, pp. 228–236, 2019.

[54] H. M. Albishri and H. M. Marwani, "Chemically modified activated carbon with tris(hydroxymethyl)aminomethane for selective adsorption and determination of gold in water samples," *Arabian Journal of Chemistry*, vol. 9, pp. 252–258, 2016.

[55] G. T. Gebremichael, H. Kim, G. M. Nisola, and W. J. Chung, "Asparagine anchored on mesoporous silica for Au (III) capture: elucidation of adsorption-reduction mechanisms and their implications towards selective Au (III) recovery," *Applied Surface Science*, vol. 567, Article ID 150743, 2021.

[56] Z. Jia, P. Yin, Z. Yang et al., "Triphosphonic acid modified multi-walled carbon nanotubes for gold ions adsorption," *Phosphorus, Sulfur, and Silicon and the Related Elements*, vol. 196, no. 2, pp. 106–118, 2020.

[57] L. Tofan, I. Bunia, C. Paduraru, and C. Teodosiu, "Synthesis, characterization and experimental assessment of a novel functionalized macroporous acrylic copolymer for gold separation from wastewater," *Process Safety and Environmental Protection*, vol. 106, pp. 150–162, 2017.

[58] K. Deng, P. Yin, X. Liu, Q. Tang, and R. Qu, "Modeling, analysis and optimization of adsorption parameters of Au(III) using low-cost agricultural residuals buckwheat hulls," *Journal of Industrial and Engineering Chemistry*, vol. 20, no. 4, pp. 2428–2438, 2014.

[59] F. Liu, Z. Zhou, and G. Li, "Persimmon tannin functionalized polyacrylonitrile fiber for highly efficient and selective recovery of Au(III) from aqueous solution," *Chemosphere*, vol. 264, Article ID 128469, 2021.

[60] Y. L. Liang, C. Jin, J. T. Hu et al., "A highly efficient pathway to recover gold from acid aqueous solution by using an amidoxime-functionalized UHMWPE fiber," *Rare Metals*, vol. 38, no. 11, pp. 1105–1112, 2019.

[61] S. Y. Hashemi, M. Yegane Badi, H. Pasalari, A. Azari, H. Arfaeinia, and A. Kiani, "Degradation of Ceftriaxone from aquatic solution using a heterogeneous and reusable O_3/UV/Fe_3O_4@TiO_2 systems: operational factors, kinetics and mineralisation," *International Journal of Environmental Analytical Chemistry*, vol. 102, pp. 6904–6920, 2022.

[62] M. Gurung, B. B. Adhikari, S. Morisada et al., "N-aminoguanidine modified persimmon tannin: a new sustainable material for selective adsorption, preconcentration and recovery of precious metals from acidic chloride solution," *Bioresource Technology*, vol. 129, pp. 108–117, 2013.

[63] W. Zhang, L. Wu, X. Han et al., "Green chemical synthesis of new chelating fiber and its mechanism for recovery gold from aqueous solution," *Journal of Hazardous Materials*, vol. 378, Article ID 120674, 2019.

[64] S. Basu, G. Ghosh, and S. Saha, "Adsorption characteristics of phosphoric acid induced activation of bio-carbon: equilibrium, kinetics, thermodynamics and batch adsorber design," *Process Safety and Environmental Protection*, vol. 117, pp. 125–142, 2018.

[65] H. Pasalari, H. R. Ghaffari, A. H. Mahvi, M. Pourshabanian, and A. Azari, "Activated carbon derived from date stone as natural adsorbent for phenol removal from aqueous solution," *https://www.crossref.org/webDeposit/*, vol. 72, pp. 406–417, 2017.

[66] M. Zhao, J. Zhao, Z. Huang, S. Wang, and L. Zhang, "One pot preparation of magnetic chitosan-cystamine composites for selective recovery of Au(III) from the aqueous solution," *molInternational Journal of Biological Macromolecules*, vol. 137, pp. 721–731, 2019.

[67] C. Cheng, Z. Liu, X. Li, B. Su, T. Zhou, and C. Zhao, "Graphene oxide interpenetrated polymeric composite hydrogels as highly effective adsorbents for water treatment," *RSC Advances*, vol. 4, no. 80, pp. 42346–42357, 2014.

[68] A. B. Kanagare, K. K. Singh, M. Kumar et al., "DTDGA-impregnated XAD-16 beads for separation of gold from electronic waste solutions," *Industrial and Engineering Chemistry Research*, vol. 55, no. 49, pp. 12644–12654, 2016.

[69] Z. Wang, X. Li, H. Liang, J. Ning, Z. Zhou, and G. Li, "Equilibrium, kinetics and mechanism of Au3+, Pd2+ and Ag+ ions adsorption from aqueous solutions by graphene oxide functionalized persimmon tannin," *Materials Science and Engineering: C*, vol. 79, pp. 227–236, 2017.

[70] S. J. Mousavi, M. Parvini, and M. Ghorbani, "Experimental design data for the zinc ions adsorption based on mesoporous modified chitosan using central composite design method," *Carbohydrate Polymers*, vol. 188, pp. 197–212, 2018.

[71] A. Azari, R. Nabizadeh, A. H. Mahvi, and S. Nasseri, "Magnetic multi-walled carbon nanotubes-loaded alginate for treatment of industrial dye manufacturing effluent: adsorption modelling and process optimisation by central composite face-central design," *International Journal of Environmental Analytical Chemistry*, vol. 103, pp. 1509–1529, 2023.

[72] M. K. M. Z. Hyder and B. Ochiai, "Selective recovery of Au(III), Pd(II), and Ag(I) from printed circuit boards using cellulose filter paper grafted with polymer chains bearing thiocarbamate moieties," *Microsystem Technologies*, vol. 24, no. 1, pp. 683–690, 2018.

[73] W. Wei, D. H. K. Reddy, J. K. Bediako, and Y. S. Yun, "Aliquat-336-impregnated alginate capsule as a green sorbent for selective recovery of gold from metal mixtures," *Chemical Engineering Journal*, vol. 289, pp. 413–422, 2016.

[74] M. Behbahani, F. Najafi, M. M. Amini, O. Sadeghi, A. Bagheri, and P. G. Hassanlou, "Solid phase extraction using nanoporous MCM-41 modified with 3,4-dihydroxybenzaldehyde for simultaneous preconcentration and removal of gold(III), palladium(II), copper(II) and silver(I)," *Journal of Industrial and Engineering Chemistry*, vol. 20, no. 4, pp. 2248–2255, 2014.

[75] F. Q. An, M. Li, X. D. Guo et al., "Selective adsorption of AuCl 4 − on chemically modified D301 resin with containing N/S functional polymer," *Journal of Environmental Chemical Engineering*, vol. 5, no. 1, pp. 10–15, 2017.

[76] L. Liu, S. Liu, Q. Zhang et al., "Adsorption of Au(III), Pd(II), and Pt(IV) from aqueous solution onto graphene oxide," *Journal of Chemical and Engineering Data*, vol. 58, no. 2, pp. 209–216, 2013.

[77] R. Fan, F. Xie, X. Guan, Q. Zhang, and Z. Luo, "Selective adsorption and recovery of Au(III) from three kinds of acidic systems by persimmon residual based bio-sorbent: a method for gold recycling from e-wastes," *Bioresource Technology*, vol. 163, pp. 167–171, 2014.

[78] L. Yang, F. Jia, and S. Song, "Recovery of [Au(CN) 2] − from gold cyanidation with graphene oxide as adsorbent," *Separation and Purification Technology*, vol. 186, pp. 63–69, 2017.

[79] M. Monier, M. A. Akl, and W. Ali, "Preparation and characterization of selective phenyl thiosemicarbazide modified Au(III) ion-imprinted cellulosic cotton fibers," *Journal of Applied Polymer Science*, vol. 131, no. 18, pp. 9277–9287, 2014.

[80] A. Asfaram, M. Ghaedi, F. Yousefi, and M. Dastkhoon, "Experimental design and modeling of ultrasound assisted simultaneous adsorption of cationic dyes onto ZnS: Mn-NPs-AC from binary mixture," *Ultrasonics Sonochemistry*, vol. 33, pp. 77–89, 2016.

[81] A. Azari, R. Nabizadeh, A. H. Mahvi, and S. Nasseri, "Integrated Fuzzy AHP-TOPSIS for selecting the best color removal process using carbon-based adsorbent materials: multicriteria decision making vs. systematic review approaches and modeling of textile wastewater treatment in real conditions," *International Journal of Environmental Analytical Chemistry*, vol. 102, pp. 7329–7344, 2022.

[82] A. N. Ebelegi, N. Ayawei, and D. Wankasi, "Interpretation of adsorption thermodynamics and kinetics," *Open Journal of Physical Chemistry*, vol. 10, no. 3, pp. 166–182, 2020.

[83] H. N. Tran, S. J. You, and H. P. Chao, "Thermodynamic parameters of cadmium adsorption onto orange peel calculated from various methods: a comparison study," *Journal of Environmental Chemical Engineering*, vol. 4, no. 3, pp. 2671–2682, 2016.

[84] Y. Cantu, A. Remes, A. Reyna et al., "Thermodynamics, kinetics, and activation energy studies of the sorption of chromium(III) and chromium(VI) to a Mn3O4 nanomaterial," *Chemical Engineering Journal*, vol. 254, pp. 374–383, 2014.

[85] S. Zhou, W. Xu, C. Hu, P. Zhang, and K. Tang, "Fast and effective recovery of Au(III) from aqueous solution by a N-containing polymer," *Chemosphere*, vol. 260, Article ID 127615, 2020.

[86] Z. Wang, B. Zhang, C. Ye, and L. Chen, "Recovery of Au(III) from leach solutions using thiourea functionalized zeolitic

imidazolate frameworks (TU*ZIF-8)," *Hydrometallurgy*, vol. 180, pp. 262–270, 2018.

[87] R. Navarro, M. A. Lira, I. Saucedo, A. Alatorre, and E. Guibal, "Amberlite XAD-1180 impregnation with Cyphos IL101 for the selective recovery of precious metals from HCl solutions," *Gold Bulletin*, vol. 50, no. 1, pp. 7–23, 2017.

[88] M. A. Zazouli, A. Azari, S. Dehghan, and R. Salmani Malekkolae, "Adsorption of methylene blue from aqueous solution onto activated carbons developed from eucalyptus bark and Crataegus oxyacantha core," *Water Science and Technology*, vol. 74, pp. 2021–2035, 2016.